Higher-order expansion of misfit functional for defect identification in elastic solids

Marc Bonnet, Rémi Cornaggia

Higher-order expansion of misfit functional for defect identification in elastic solids

Marc Bonnet[1], **Rémi Cornaggia**[1,*]
[1]Poems (UMR 7231 CNRS-INRIA-ENSTA), Palaiseau, France
[*]Email: remi.cornaggia@ensta-paristech.fr

Abstract. In this work, least-squares functionals commonly used for defect identification are expanded in powers of the small radius of a trial inclusion, in the context of time-harmonic elastodynamics, generalizing to higher orders the concept of topological derivative. Such expansion, whose derivation and evaluation are facilitated by using an adjoint state, provides a basis for the quantitative estimation of flaws whereby a region of interest may be exhaustively probed at reasonable computational cost.

Keywords: Topological derivative, identification, elastodynamics, asymptotic analysis

Problem statement. We consider a reference (i.e defect-free) 3D elastic solid Ω characterized by Hooke's tensor $\boldsymbol{\mathcal{C}}$ and mass density ρ. The time-harmonic background displacement $\boldsymbol{u}$ then solves

$$\langle \boldsymbol{u}, \boldsymbol{w}\rangle_\Omega^{\mathcal{C}} - \omega^2(\boldsymbol{u},\boldsymbol{w})_\Omega^\rho = \mathcal{F}(\boldsymbol{w})\ \forall \boldsymbol{w}\in\mathcal{W}, \quad (1)$$

where $\langle .,.\rangle_D^{\mathcal{C}}$ and $(.,.)_D^\rho$ denote the stiffness and mass bilinear forms associated to a given domain D characterized by $(\boldsymbol{\mathcal{C}},\rho)$, $\mathcal{W}\subset H^1(\Omega)$ is the function space incorporating the relevant essential boundary conditions (if any), the linear form $\mathcal{F}\in\mathcal{W}'$ defines the applied time-harmonic loading and ω is the angular frequency.

Assuming the presence of a defect inside Ω, and that we can measure the resulting displacement $\boldsymbol{u}^{\text{ex}}$ on a surface Γ, we define the least-squares cost functional $J(\boldsymbol{w})$, with the elastodynamic displacement $\boldsymbol{w}$ associated to the given excitation and a known trial defect, by:

$$J(\boldsymbol{w}) = \frac{1}{2}\int_\Gamma |\boldsymbol{w}(\boldsymbol{x}) - \boldsymbol{u}^{\text{ex}}(\boldsymbol{x})|^2\,\mathrm{d}S_{\boldsymbol{x}} \quad (2)$$

We now consider a specific trial defect $B_a = \boldsymbol{z}+a\mathcal{B}$ (Fig 1), centered at $\boldsymbol{z}\in\Omega$, of small size a and reference shape $\mathcal{B}$. It is a perfectly bonded inclusion filled with a material characterized by its Hooke tensor $\boldsymbol{\mathcal{C}}^\star = \boldsymbol{\mathcal{C}}+\Delta\boldsymbol{\mathcal{C}}$ and mass density $\rho^\star = \rho+\Delta\rho$. We denote $\boldsymbol{u}_a$ the displacement in the perturbed domain, and $\boldsymbol{v}_a = \boldsymbol{u}_a - \boldsymbol{u}$ the displacement perturbation. $J(\boldsymbol{u}_a)$ admits the exact expansion about $\boldsymbol{u}$:

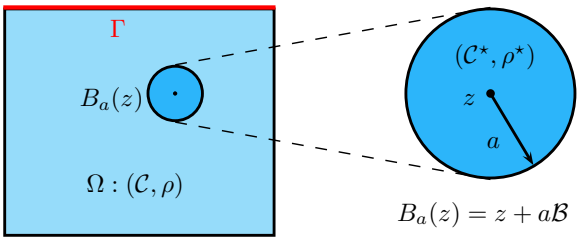

Figure 1: Computational domain and inclusion.

$$\begin{aligned} J(\boldsymbol{u}_a) &= J(\boldsymbol{u}) + J'(\boldsymbol{u};\boldsymbol{v}_a) + J''(\boldsymbol{u};\boldsymbol{v}_a,\boldsymbol{v}_a) \\ &= J(\boldsymbol{u}) + \Re\int_\Gamma \overline{(\boldsymbol{u}-\boldsymbol{u}^{\text{ex}})}\cdot\boldsymbol{v}_a + \frac{1}{2}\int_\Gamma |\boldsymbol{v}_a|^2 \end{aligned} \quad (3)$$

The goal is now to expand $J(\boldsymbol{u}_a)$ in powers of a. Similar expansions have been studied in e.g. [2] for rigid obstacles in 3D acoustic media and [5] for holes in 2D elastic bodies.

Define the adjoint field $\boldsymbol{p}$ as the solution of

$$\langle \boldsymbol{p}, \boldsymbol{w}\rangle_\Omega^{\mathcal{C}} - \omega^2(\boldsymbol{p},\boldsymbol{w})_\Omega^\rho = J'(\boldsymbol{u};\boldsymbol{w})\ \forall \boldsymbol{w}\in\mathcal{W}. \quad (4)$$

We can then compute $J'(\boldsymbol{u};\boldsymbol{v}_a)$ as

$$J'(\boldsymbol{u};\boldsymbol{v}_a) = -\langle \boldsymbol{p}, \boldsymbol{u}_a\rangle_{B_a}^{\Delta\mathcal{C}} + \omega^2(\boldsymbol{p},\boldsymbol{u}_a)_{B_a}^{\Delta\rho} \quad (5)$$

Expanding $\boldsymbol{v}_a$ in powers of a is now needed. As we will see, $J''(\boldsymbol{u};\boldsymbol{v}_a,\boldsymbol{v}_a)$ requires only the leading contribution of $\boldsymbol{v}_a|_\Gamma$ whereas a higher-order expansion of $\boldsymbol{v}_a|_{B_a}$ is needed for evaluating (5).

Expansion of the solution perturbation. Following e.g. [3], $\boldsymbol{v}_a$ solves the integro-differential Lippmann-Schwinger equation:

$$\mathcal{L}_a[\boldsymbol{v}_a](\boldsymbol{x}) = -\langle \boldsymbol{u}, \boldsymbol{G}\rangle_{B_a}^{\Delta\mathcal{C}} + \omega^2(\boldsymbol{u},\boldsymbol{G})_{B_a}^{\Delta\rho} \quad (6)$$

with $\mathcal{L}_a[\boldsymbol{v}](\boldsymbol{x}) := \boldsymbol{v}(\boldsymbol{x}) + \langle \boldsymbol{v}, \boldsymbol{G}\rangle_{B_a}^{\Delta\mathcal{C}} - \omega^2(\boldsymbol{v},\boldsymbol{G})_{B_a}^{\Delta\rho}$ and $\boldsymbol{G} = \boldsymbol{G}(\cdot,\boldsymbol{x})$ is the elastodynamic Green's tensor for a unit point force applied at $\boldsymbol{x}$ and satisfying homogeneous boundary conditions consistent with problem (1) on $\partial\Omega$. Substituting the ansatz

$$\begin{aligned} \boldsymbol{v}_a(\boldsymbol{x}) = a\boldsymbol{V}_1(\bar{\boldsymbol{x}}) + a^2\boldsymbol{V}_2(\bar{\boldsymbol{x}}) + \tfrac{1}{2}a^3\boldsymbol{V}_3(\bar{\boldsymbol{x}}) \\ + \tfrac{1}{6}a^4\boldsymbol{V}_4(\bar{\boldsymbol{x}}) + \boldsymbol{\delta}_a(\boldsymbol{x}), \qquad \boldsymbol{x}\in B_a \end{aligned} \quad (7)$$

(with $\bar{\boldsymbol{x}} := (\boldsymbol{x}-\boldsymbol{z})/a \in \mathcal{B}$) into (6) and expanding the resulting equation in powers of a (in particular using that $\boldsymbol{G}(\boldsymbol{\xi},\boldsymbol{x}) = a^{-1}\boldsymbol{G}_\infty(\bar{\boldsymbol{\xi}}-\bar{\boldsymbol{x}})+O(1)$, with $\boldsymbol{G}_\infty$ denoting the *static* full-space Kelvin fundamental solution) yields a sequence of integral equations for the $\boldsymbol{V}_j$. These equations correspond to *elastostatic* problems for the normalized inclusion $\mathcal{B}$ embedded in an unbounded reference medium, and are solved with the help of Eshelby's equivalent inclusion method [4].

The remainder $\boldsymbol{\delta}_a$ in (7) solves an integro-differential equation of the form $\mathcal{L}_a[\boldsymbol{\delta}_a] = \boldsymbol{\gamma}_a$. The operator $\mathcal{L}_a : H^1(B_a) \to H^1(B_a)$ is shown to be invertible with bounded inverse, while $\boldsymbol{\gamma}_a$ can be estimated as $\|\boldsymbol{\gamma}_a\|_{H^1(B_a)} = O(a^{11/2})$. Consequently, there exists a constant $C > 0$ independent of a such that

$$\|\boldsymbol{\delta}_a\|_{H^1(B_a)} \leq C a^{11/2}. \tag{8}$$

For $\boldsymbol{x} \notin B_a$, plugging (7) in the form $\boldsymbol{v}_a(\boldsymbol{x}) \approx a\boldsymbol{V}_1(\bar{\boldsymbol{x}})$ into (6) yields the outer expansion

$$\begin{aligned}\boldsymbol{v}_a(\boldsymbol{x}) = -a^3\big[\,&\boldsymbol{\nabla}\boldsymbol{u}(\boldsymbol{z}):\boldsymbol{\mathcal{A}}:\boldsymbol{\nabla}\boldsymbol{G}(\boldsymbol{z},\boldsymbol{x}) \\ &- \omega^2\Delta\rho|\mathcal{B}|\boldsymbol{u}(\boldsymbol{z})\cdot\boldsymbol{G}(\boldsymbol{z},\boldsymbol{x})\,\big] + o(a^3),\end{aligned} \tag{9}$$

$\boldsymbol{\mathcal{A}}$ being the elastic moment tensor associated to $\mathcal{B}$, $\boldsymbol{\mathcal{C}}$ and $\Delta\boldsymbol{\mathcal{C}}$ [1,3].

Cost functional expansion. Substituting (7) into (5) and (9) into (3), $J(\boldsymbol{u}_a)$ is finally found to have an expansion of the form:

$$J(\boldsymbol{u}_a) = J_6(a,\boldsymbol{z}) + o(a^6) \tag{10}$$

$$\begin{aligned}\text{with}\quad J_6(a,\boldsymbol{z}) = J(\boldsymbol{u}) &+ a^3\mathcal{T}_3(\boldsymbol{z}) + a^4\mathcal{T}_4(\boldsymbol{z}) \\ &+ a^5\mathcal{T}_5(\boldsymbol{z}) + a^6\mathcal{T}_6(\boldsymbol{z}),\end{aligned}$$

the $o(a^6)$ estimate resulting from (8) and (9).

The $\mathcal{T}_j(\boldsymbol{z})$ are found to be given in terms of (i) the background field $\boldsymbol{u}$ and its derivatives at $\boldsymbol{z}$, (ii) the adjoint field $\boldsymbol{p}$ and its derivatives at $\boldsymbol{z}$, (iii) $\boldsymbol{\mathcal{A}}$ and other elastic moment tensors that involve the material parameters, the shape $\mathcal{B}$ and the angular frequency ω, and (iv) the complementary part of $\boldsymbol{G}$, i.e. $\boldsymbol{G} - \boldsymbol{G}_\infty = (\boldsymbol{G}_{\infty,\omega}-\boldsymbol{G}_\infty)+\boldsymbol{G}_C$, where $\boldsymbol{G}_{\infty,\omega}$ is the elastodynamic full-space fundamental solution and $\boldsymbol{G}_C$ accounts for the boundedness of Ω. In particular, $\mathcal{T}_3(\boldsymbol{z})$ is the well-known topological derivative:

$$\mathcal{T}_3(\boldsymbol{z}) = -\big[\,\boldsymbol{\nabla}\boldsymbol{u}:\boldsymbol{\mathcal{A}}:\boldsymbol{\nabla}\boldsymbol{p} - \omega^2\Delta\rho|\mathcal{B}|\boldsymbol{u}\cdot\boldsymbol{p}\,\big](\boldsymbol{z}).$$

Moreover, $\mathcal{T}_4(\boldsymbol{z}) = 0$ for any centrally-symmetric shape $\mathcal{B}$. The complementary part $\boldsymbol{G}_{\infty,\omega} - \boldsymbol{G}_\infty$ (known analytically) is involved in $\mathcal{T}_5(\boldsymbol{z})$ and $\mathcal{T}_6(\boldsymbol{z})$, while $\boldsymbol{G}_C$ appears in $\mathcal{T}_6(\boldsymbol{z})$ only. Since the exact computation of $\boldsymbol{G}_C$ would require solving an elastodynamic problem on Ω for each trial location $\boldsymbol{z}$, we plan to use an approximation method to save computational time.

Closed-form formulae for the $\mathcal{T}_j$ can be obtained when $\mathcal{B}$ is spherical (for which case we provide explicit expressions) or ellipsoidal.

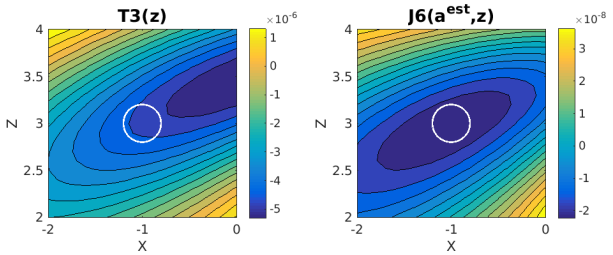

Figure 2: $\mathcal{T}_3(\boldsymbol{z})$ and $J_6(a^{\text{est}},\boldsymbol{z})$ plotted in the (XZ) plane around the obstacle (in white).

Identification. Following [2], estimates of the location $\boldsymbol{z}^{\text{est}}$ and size a^{est} of the real defect can then be sought as minimizers of $J_6(a,\boldsymbol{z})$, with $\boldsymbol{z}$ spanning a predefined sampling grid. This entails computing the $\mathcal{T}_j(\boldsymbol{z})$ over the sampling grid and minimizing $a \mapsto J_6(a,\boldsymbol{z})$ for each $\boldsymbol{z}$, the latter step being very fast and straightforward

A preliminary example is set in free space (so that $\boldsymbol{G}_C = 0$) for a spherical scatterer of radius $0.1\lambda_S$ illuminated by a plane P-wave travelling along the positive x-direction, with a discrete array of displacement sensors lying behind the scatterer. The above procedure yields the size estimate $a^{\text{est}} \approx 0.105\lambda_S$; moreover, the estimated location $\boldsymbol{z}^{\text{est}}$ is found to be very close to the true center of the scatterer. The contour plot of $J_6(a^{\text{est}},\boldsymbol{z})$ (Fig 2) shows improved localisation (relative to the topological derivative $\mathcal{T}_3(\boldsymbol{z})$) for this partial-aperture configuration.

References

[1] H. Ammari and H. Kang. *Polarization and moment tensors.* Springer, 2007.

[2] M. Bonnet. Inverse acoustic scattering by small-obstacle expansion of a misfit function. *Inverse Problems*, 24(3):035022, 2008.

[3] M. Bonnet and G. Delgado. The topological derivative in anisotropic elasticity. *Quart. J. Mech. Appl. Math.*, 66:557–586, 2013.

[4] T. Mura. *Micromechanics of defects in solids.* M. Nijhoff Publishers, 1982.

[5] M. Silva, M. Matalon, and D. A. Tortorelli. Higher order topological derivatives in elasticity. *Int J Solids Struct.*, 47:3053 – 3066, 2010.